ARTICLE

OBC
www.rsc.org/obc

Ketene-forming eliminations from aryl bis(4′-chlorophenyl)acetates promoted by R_2NH–$R_2NH_2^+$ in aqueous MeCN. Change of mechanism †

Sang Yong Pyun,[a] Dong Choon Lee,[a] Ju Chang Kim[a] and Bong Rae Cho*[b]

[a] *Department of Chemistry, Pukyong National University, Pusan 608-737, Korea*

[b] *Department of Chemistry, Korea University, 1-Anamdong, Seoul 136-701, Korea. E-mail: chobr@korea.ac.kr*

Received 25th March 2003, Accepted 11th June 2003
First published as an Advance Article on the web 23rd June 2003

Elimination reactions of $(4'\text{-}ClC_6H_4)_2CHCO_2C_6H_3\text{-}2\text{-}X\text{-}4\text{-}NO_2$ promoted by R_2NH–$R_2NH_2^+$ in 70 mol% MeCN (aq.) have been studied kinetically. The reactions are second-order and exhibit Brönsted $\beta = 0.44$–0.86 and $|\beta_{lg}| = 0.41$–0.71. The Brönsted β decreased with a poorer leaving group and $|\beta_{lg}|$ increased with a weaker base. The results are consistent with an E2 mechanism. When X = H, the reaction proceeded by the concurrent E2 and E1cb mechanism.

Introduction

Ketene-forming eliminations from aryl phenylacetates have been extensively investigated because of the mechanistic diversity in the E2 and E1cb borderline. It is well known that base-catalyzed hydrolysis of *p*-nitrophenylacetates and other esters proceed by an E1cb mechanism to afford the ketene intermediate followed by the addition of water.[1–14] When R_2NH in MeCN was used as the base-solvent system, the reaction proceeded by the E2 mechanism *via* an E1cb-like transition state.[15,16] A competing E2 and E1cb mechanism was observed in eliminations from *p*-nitrophenyl *p*-nitrophenylacetates promoted by R_2NH–$R_2NH_2^+$ in 70 mol% MeCN (aq.).[15] Moreover, a gradual change of the mechanism from E2 to E1cb *via* a competing E2 and E1cb mechanism has been demonstrated by systematically varying the structure of $2\text{-}Y\text{-}4\text{-}NO_2C_6H_3CH_2CO_2C_6H_3\text{-}2\text{-}X\text{-}4\text{-}NO_2$.[17] The transition state gradually became more E1cb-like as a poorer leaving group was introduced, and the E1cb mechanism emerged when X, Y = H. The E1cb mechanism became predominant when X = H and Y = NO_2, probably because the carbanion intermediate was stabilized by the strongly electron-withdrawing substituent and the E2 mechanism could no longer compete.

Recently, we reported that the ketene-forming elimination from Ph_2CHCO_2Ar promoted by R_2NH–$R_2NH_2^+$ in 70 mol% MeCN (aq.) proceeded *via* an E2-central transition state, with similar extents of C_β–H and C_α–OAr bond cleavage.[18] Comparison of the transition state parameters revealed that the extent of proton transfer decreased and the degree of the leaving group bond cleavage increased by the change of the substrate from $PhCH_2CO_2Ar$ to Ph_2CHCO_2Ar. The result was attributed to the double bond stabilizing effect of the β-Ph group. To further expand our understanding of ketene-forming eliminations, we have now studied the reactions of aryl bis(4′-chlorophenyl)acetates **1a**–**d** under the same condition (eqn. 1).

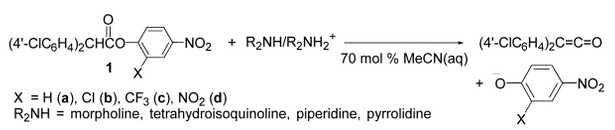

(1)

We were interested in learning if a change to the E1cb mechanism could be realized from the E2-central transition state by introducing an electron withdrawing substituent at the β–aryl group. Here we report that the elimination reactions from **1b**–**d** proceed by the E2 mechanism *via* an E2-central transition state. When the leaving group was changed to X = H (**1a**), the mechanism changed to a competing E2 and E1cb. By comparing with the existing data for Ph_2CHCO_2Ar, the effect of β–aryl substituent on the ketene-forming elimination is assessed.

Results

For reactions of **1a**–**d** with R_2NH–$R_2NH_2^+$ in 70 mol% MeCN (aq.), the yields of aryloxides as determined by comparison of the UV absorption of the infinity sample of the kinetic runs with those of the authentic aryloxides were in the range 90–98%. The possibility of a competing aminolysis had been ruled out in a previous study.[18] The rates of elimination reactions were followed by monitoring the increase in the absorption at the λ_{max} for the aryloxides in the range of 400–426 nm. In all cases, clean isosbestic points were noted in the range 310–312 nm. Excellent pseudo-first-order kinetics plots which covered at least three half-lives were obtained.

The plots of k_{obs} *vs.* base concentration for the reaction of **1b**–**d** are straight lines passing through the origin, indicating that the reactions are second-order, first order to the substrate and first order to the base (Fig. 1 and Figs S1 and S2 in the ESI †). The slopes are the overall second-order rate constants k_2^E. Values of k_2^E for eliminations from **1b**–**d** are summarized in Table 1.

On the other hand, the plots of k_{obs} *vs* [base] for the reactions of **1a** with R_2NH–$R_2NH_2^+$ in 70 mol% MeCN (aq.) showed curvilinear relationships (Fig. 2 and S3–S6 †). The data were analyzed by assuming that the reaction proceeds by concurrent E2 and E1cb mechanisms (eqn. 2).[15,17] The k_2^E, k_1, and k_{-1}/k_2 values that best fit with eqn. 2 were calculated, and the plots were dissected into the E2 and E1cb reaction components.[20] In all cases, the correlations between the calculated and the

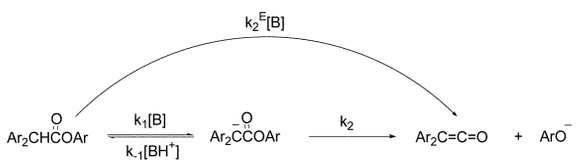

(2)

† Electronic supplementary information (ESI) available: Rate constants for eliminations from **1a**–**d** promoted by R_2NH–$R_2NH_2^+$ in 70 mol% MeCN (aq.), plots of k_{obs} *vs* base concentration, and plots of log k_1 and log k_{-1}/k_2 *vs* pK_a. See http://www.rsc.org/suppdata/ob/b3/b303231k/

DOI: 10.1039/b303231k

Table 1 Rate constants for ketene-forming eliminations from $(4'\text{-}ClC_6H_4)_2CHCO_2C_6H_3$-2-X-4-$NO_2$ [a] (**1a**–**d**) Promoted by R_2NH–$R_2NH_2^+$ in 70 mol% MeCN (aq.) [b,c] at 25.0 °C

		$k_2^E/M^{-1}\ s^{-1}$ [f,g]			
R_2NH [d]	pK_a [e]	X = H (**1a**) [h]	X = Cl (**1b**)	X = CF_3 (**1c**)	X = NO_2 (**1d**)
Morpholine	16.6	0.0111	0.531	2.57	17.6
THIQ [i]	17.1	0.0165	1.08	5.10	36.9
Piperidine	18.9	0.310 [j]	10.7	39.4	198
Pyrrolidine	19.6	5.53	67.9	212	410

[a] [Substrate] = 3.0×10^{-5} M. [b] $[R_2NH]/[R_2NH_2^+] = 1.0$. [c] $\mu = 0.10$ M ($Bu_4N^+Br^-$). [d] $[R_2NH] = 6.0 \times 10^{-4}$ to 2.0×10^{-1} M. [e] Ref. 18. [f] Average of three or more rate constants. [g] Estimated uncertainty, ± 5%. [h] Calculated from the k_{obs} by using eqn. 2. [i] Tetrahydroisoquinoline. [j] $k_2^E = 0.325\ M^{-1}\ s^{-1}$ when $[R_2NH]/[R_2NH_2^+] = 0.5$.

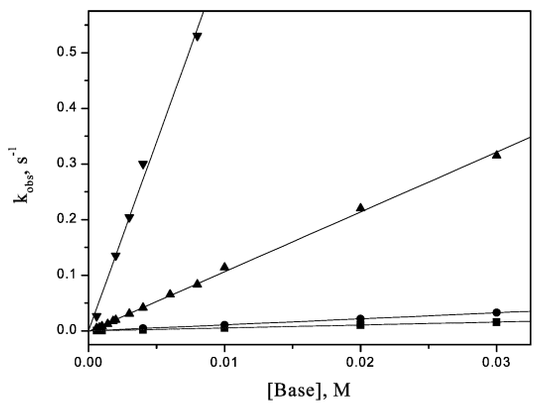

Fig. 1 Plots of k_{obs} *vs* base concentration for eliminations from $(4'\text{-}ClC_6H_4)_2CHCO_2C_6H_3$-2-Cl-4-$NO_2$ (**1b**) promoted by R_2NH–$R_2NH_2^+$ in 70 mol% MeCN (aq.) at 25.0 °C, $[R_2NH]/[R_2NH_2^+] = 1.0$, $\mu = 0.10$ M ($Bu_4N^+Br^-$). R_2NH = morpholine (■), tetrahydroisoquinoline (●), piperidine (▲), pyrrolidine (▼).

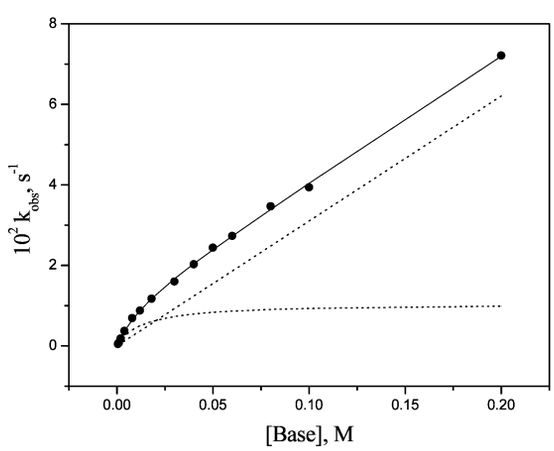

Fig. 2 Plot of k_{obs} *vs* buffer concentration for eliminations from $(4'\text{-}ClC_6H_4)_2CHCO_2C_6H_4$-4-$NO_2$ (**1a**) promoted by R_2NH–$R_2NH_2^+$ in 70 mol% MeCN (aq.) at 25.0 °C, $[R_2NH]/[R_2NH_2^+] = 1.0$, $\mu = 0.10$ M ($Bu_4N^+Br^-$), R_2NH = Piperidine. The closed circles are the experimental data and the solid line shows the computer fitted curve by using eqn. 2. The curve is dissected into the E2 and E1cb reaction components (dashed lines).

experimental data are excellent. Calculated values of k_2^E, k_1, and k_{-1}/k_2 for the eliminations from **1a** are summarized in Tables 1 and 2.

The possibility of the buffer association as the cause of the curvature was ruled out by the straight lines observed in the plots of k_{obs} *vs* [base] for the reaction of **1b**–**d** (Fig 1, S1 and S2 †). Also, the possibility that the salt effect may have caused the increase in the k_{obs} at higher base concentration is negated because the ionic strength is maintained to be 0.1 M with $Bu_4N^+Br^-$. To assess the effect of buffer ratio, the k_{obs} values for the ketene-forming eliminations from **1a** have also been measured at $[R_2NH]/[R_2NH_2^+] = 0.5$. At a given base concentration,

Table 2 The k_1 and k_{-1}/k_2 values for ketene-forming eliminations from $(4'\text{-}ClC_6H_4)_2CHCO_2C_6H_4$-4-$NO_2$ (**1a**) [a] Promoted by R_2NH–$R_2NH_2^+$ buffers in 70 mol% MeCN (aq.) [b,c] at 25.0 °C

R_2NH [d]	$k_1/M^{-1}\ s^{-1}$ [e,f]	$k_{-1}/k_2/M^{-1}$ [e,g]
Morpholine	0.123	1590
THIQ [h]	0.168	730
Piperidine [i]	0.792	74.6
Pyrrolidine	2.02	26.7

[a] [Substrate] = 3.0×10^{-5} M. [b] $[R_2NH]/[R_2NH_2^+] = 1.0$ except otherwise noted. [c] $\mu = 0.10$ M ($Bu_4N^+Br^-$). [d] $[R_2NH] = 6.0 \times 10^{-4}$ to 2.0×10^{-1} M. [e] Calculated from the k_{obs} by using eqn. 2. [f] The slope of the plot of log k_1 *vs* pK_a of the base is 0.40 ± 0.03. [g] The slope of the plot of log k_{-1}/k_2 *vs* pK_a of the base is −0.58 ± 0.01. [h] Tetrahydroisoquinoline. [i] $k_1 = 0.755\ M^{-1}\ s^{-1}$ and $k_{-1}/k_2 = 77.9\ M^{-1}$, respectively, when $[R_2NH]/[R_2NH_2^+] = 0.5$.

the k_{obs} is always smaller at a lower buffer ratio, as expected from eqn. 2 (Table S1 †). Moreover, the rate data show excellent correlation with eqn. 2 and the calculated values of k_2^E, k_1, and k_{-1}/k_2 for the piperidine-promoted eliminations from **1a** are nearly identical regardless of the buffer ratio (see footnote in Tables 1 and 2). These results provide additional evidence in support of the kinetic analysis given above.

The Brönsted plots for the R_2NH–promoted eliminations from **1a**–**d** are linear with excellent correlations (Fig. 3). The β values are in the range of 0.44–0.86 and increase with poorer leaving groups and as the electron-withdrawing ability of the β-aryl substituent increases (Table 3). Similarly, the k_2^E values correlated satisfactorily with the leaving group pK_{lg} values (Fig. 4). The $|\beta_{lg}|$ values are in the range of 0.41–0.71 and increase with a weaker base and remain nearly the same with the variation of the β-aryl substituent (Tables 4 and 5).

For reactions of **1a** with R_2NH–$R_2NH_2^+$ in 70 mol% MeCN (aq.), the k_1 increases and the k_{-1}/k_2 decreases with a stronger

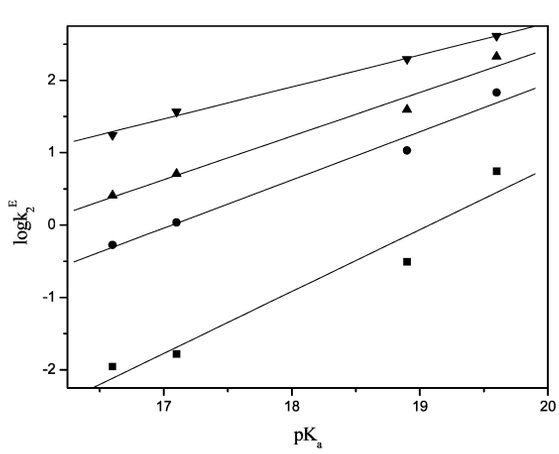

Fig. 3 Brönsted plots for the ketene-forming eliminations from $(4'\text{-}ClC_6H_4)_2CHCO_2C_6H_3$-2-X-4-$NO_2$ (**1a**–**d**) promoted by R_2NH–$R_2NH_2^+$ in 70 mol% MeCN (aq.) at 25.0 °C, $[R_2NH]/[R_2NH_2^+] = 1.0$, $\mu = 0.10$ M ($Bu_4N^+Br^-$). [X = H (**1a**, ■), Cl (**1b**, ●), CF_3 (**1c**, ▲), NO_2 (**1d**, ▼)].

Table 3 Brönsted β values for ketene-forming eliminations from (4′-$ClC_6H_4)_2CHCO_2C_6H_3$-2-X-4-NO_2 (**1a–d**) promoted by R_2NH–$R_2NH_2^+$ in 70 mol% MeCN (aq.) at 25.0 °C

X	H	Cl	CF_3	NO_2
pK_{lg}[a]	20.7	18.1	17.0	16.0
β	0.86 ± 0.14	0.67 ± 0.07	0.60 ± 0.06	0.44 ± 0.02

[a] Ref. 17.

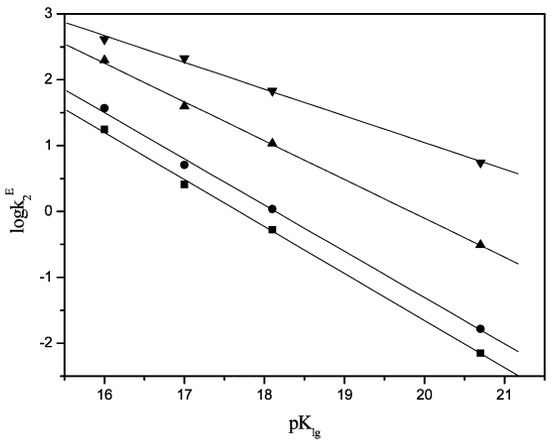

Fig. 4 Plots of log k_2^E *vs* pK_{lg} values of the leaving group for eliminations from (4′-$ClC_6H_4)_2CHCO_2C_6H_3$-2-X-4-NO_2 (**1a–d**) promoted by R_2NH–$R_2NH_2^+$ in 70 mol% MeCN (aq.) at 25.0 °C, $[R_2NH]/[R_2NH_2^+] = 1.0$, $\mu = 0.10$ M ($Bu_4N^+Br^-$). [R_2NH = morpholine (■), tetrahydroisoquinoline (●), piperidine (▲), pyrrolidine (▼)].

base (Table 2). The plots of log k_1 and log k_{-1}/k_2 *vs* the pK_a values of $R_2NH_2^+$ are straight lines with excellent correlation (Figs S7, S8†). The slopes of the plots are 0.40 ± 0.03 and −0.58 ± 0.01, respectively.

To provide additional evidence for the competing E1cb mechanism, an H–D exchange experiment was carried out by mixing **1a** with R_2NH–$R_2NH_2^+$ in 70 mol% MeCN–30% D_2O at −10 °C. The reactant was recovered immediately after mixing. The NMR spectrum indicated that approximately 10% of the benzylic C–H bond of **1a** was converted to a C–D bond.

Discussion

Mechanism of eliminations from 1a–d

Results of kinetic investigations and product studies reveal that the reactions of **1b–d** with R_2NH–$R_2NH_2^+$ in 70 mol% MeCN (aq.) proceed by the E2 mechanism. Because the possibility of competing aminolysis is ruled out,[18] and the ketene-forming elimination reactions exhibit second-order kinetics, all but bimolecular pathways can be ruled out. Moreover, an E1cb mechanism is negated by the substantial values of β and $|\beta_{lg}|$.[21–23] The positive interaction coefficients, *i.e.*, $p_{xy} = \partial\beta/\partial pK_{lg} = \partial\beta_{lg}/\partial pK_{BH} > 0$, provide additional evidence for the E2 mechanism (*vide infra*).[23–25]

On the other hand, the plots of k_{obs} *vs* base concentration for the reactions of **1a** are curves at low buffer concentration and straight lines at [base] > 0.01–0.05 M (Fig. 2 and S3–S6†). Similar results were observed in eliminations from *p*-nitrophenyl *p*-nitrophenylacetates under the same conditions and were ascribed to the concurrent E2 and E1cb mechanisms, *i.e.*, $k_{obs} = k_2^E + k_1k_2[B]/(k_{-1}[BH^+] + k_2)$ (eqn. 2).[15,17] Hence, the present result can also be attributed to the same mechanism. There is convincing evidence in support of this mechanism. (i) All of the rate data show excellent correlation with eqn. 2. Also, the shapes of the dissected curves are typical for the E2 and E1cb mechanisms. (ii) The k_{obs} decreases when buffer ratio is changed from 1.0 to 0.5, as expected from eqn. 2 (Table S1†). Moreover, the calculated values of k_2^E, k_1, and k_{-1}/k_2 are nearly the same regardless of buffer ratio, indicating that the same mechanism is operating under these conditions (see footnotes for Tables 1 and 2). (iii) The k_2^E values for **1a** nicely fit in the trend observed for **1b–d**, *i.e.*, they increase gradually with a better leaving group and a stronger base (Table 1). They show excellent correlations in the Brönsted plots (Figs 3 and 4), and the calculated values of β and $|\beta_{lg}|$ are in good agreement with the E2 mechanism (Tables 3 and 4). (iv) The k_1 increases with a stronger base, as would be expected for a deprotonation step. In addition, the slope of the plot of log k_1 *vs* pK_a of the base is 0.40 ± 0.03, which is again consistent because the transition state for this step should be reactant-like (see footnote in Table 2). (v) The increase in the k_{-1}/k_2 ratios with a weaker base is also consistent. The k_{-1} should increase with the acidity of $R_2NH_2^+$, although little change is expected for k_2 by the base strength variation. This predicts an increase in the k_{-1}/k_2 ratio with a weaker base, as observed. Furthermore, the slope of the plot of log k_{-1}/k_2 *vs* pK_a of the base is −0.58 ± 0.03. Note that the sum of the absolute values of the slopes of the plots for the k_1 and k_{-1} steps are close to unity. This is as expected, if the β value for the complete deprotonation is unity and if k_2 is a constant (*vide supra*). (vi) The NMR spectrum of the recovered reactant from the reaction of **1a** with R_2NH–$R_2NH_2^+$ in 70 mol% MeCN–30% D_2O at −10 °C indicated that approximately 10% of the benzylic C–H bonds of **1a** underwent H–D exchange.

Table 5 Effect of β-aryl substituent on the E2 reactions of (4′-$YC_6H_4)_2CHCO_2C_6H_4$-2-X-4-NO_2 promoted by R_2NH–$R_2NH_2^+$ in 70 mol% MeCN (aq.) at 25.0 °C

	Y = H[a]	Y = Cl (**1a**)
Rel. rate[b]	1	3
β[c]	0.67 ± 0.04	0.86 ± 0.14
β_{lg}	−0.57 ± 0.04	−0.59 ± 0.02

[a] Ref. 18. [b] R_2NH = piperidine. [c] X = H.

Mapping of the E2 transition state

The structures of the transition states may be assessed by the Brönsted β and $|\beta_{lg}|$ values. For R_2NH-promoted eliminations from **1d**, the value of $\beta = 0.44$ was determined (Table 3). This indicates less than half proton transfer in the transition state. The $|\beta_{lg}|$ values are usually taken as a measure of the extent of the leaving group cleavage. However, it should be noted that the values of $|\beta_{lg}|$ are not restricted to 0–1. In fact, for reactions involving loss of arenesulfonate in the rate-determining step, they range up to nearly 3.0.[26] For ketene-forming eliminations from aryl *p*-nitrophenylacetates, the maximum value of $|\beta_{lg}| = 1.34$ was reported.[8,15] Therefore, the measured values of $|\beta_{lg}| = 0.41$ for pyrrolidine-promoted eliminations from **1d** can most

Table 4 Brönsted β_{lg} values for ketene-forming eliminations from (4′-$ClC_6H_4)_2CHCO_2C_6H_3$-2-X-4-NO_2 (**1a–d**) promoted by R_2NH–$R_2NH_2^+$ in 70 mol% MeCN (aq.) at 25.0 °C

R_2NH	Morpholine	THIQ[a]	Piperidine	Pyrrolidine
pK_a[b]	16.6	17.1	18.9	19.6
β_{lg}	−0.71 ± 0.02	−0.70 ± 0.02	−0.59 ± 0.02	−0.41 ± 0.02

[a] Tetrahydroisoquinoline. [b] Ref. 18.

reasonably be interpreted with a moderate C_α–OAr bond cleavage in the transition state. Taken together, the transition state for the ketene-forming elimination from **1d** appears to be reactant-like, with less than half proton transfer and a smaller degree of the leaving group bond cleavage. Therefore, it seems reasonable to locate the transition state slightly toward the reactant from the E2-central in the More-O'Ferrall–Jencks reaction coordinate diagram (D in Fig. 5).

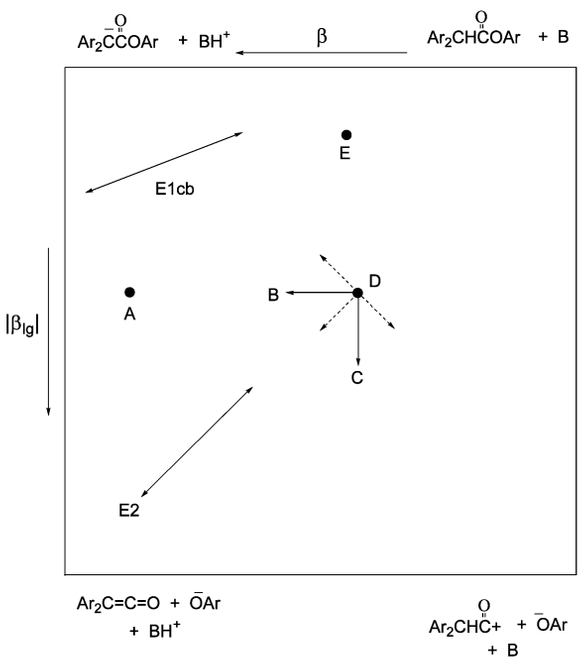

Fig. 5 Reaction coordinate diagram for the ketene-forming elimination. The effect of the change to a poorer leaving group and a weaker base are shown by the shift of the transition state from D to B and D to C, respectively. The transition states for eliminations from **1a**,**1d**, and *p*-nitrophenyl *p*-nitrophenylacetate are indicated as A, D, and E, respectively.

This conclusion is supported by the interaction coefficients. Table 3 shows that the β values of the k_2^E process for **1a**–**d** increase with a poorer leaving group. This effect corresponds to a positive p_{xy} interaction coefficient, $p_{xy} = \partial\beta/\partial pK_{lg}$, which describes the interaction between the base catalyst and the leaving group.[23–25] The observed increase in the $|\beta_{lg}|$ values with a weaker base (Table 4) is another manifestation of this effect, *i.e.*, $p_{xy} = \partial\beta_{lg}/\partial pK_{BH} > 0$. On the More-O'Ferrall–Jencks diagram in Fig. 5, a change to a poorer leaving group will raise the energy of the bottom edge of the diagram shifting the transition state toward the product and the E1cb intermediate. The transition state will then move toward the left as depicted by a shift from D to B on the energy diagram, resulting in an increase in β (Fig. 5).[23–25] A further increase in the leaving group basicity to X = H (**1a**) is expected to shift the transition state to A, in agreement with the large β. Similarly, a weaker base will raise the energy of the left side of the diagram and shift the transition state from D to C to increase the extent of C_α–OAr bond cleavage and $|\beta_{lg}|$ (Fig. 5).[23–25] The positive p_{xy} coefficients are not consistent with an E1cb mechanisms for which $p_{xy} = 0$ is expected, but provide additional support for the concerted E2 mechanism.[23–25]

Effect of β–aryl substituent on the E2 transition state

Table 5 compares the rates and transition state parameters for the E2 reactions of $(4'\text{-}YC_6H_4)_2CHCO_2C_6H_4\text{-}4\text{-}NO_2$. The rate of the E2 reaction is 3 fold faster when Y = Cl (**1a**) than when Y = H, indicating a modest increase by the *p*-Cl groups. On the other hand, Brönsted β increases and $|\beta_{lg}|$ remain nearly the same by the same variation of the substituent. The transition state for the ketene-forming elimination from **1a** is more skewed toward the proton transfer with similar extent of the leaving group bond cleavage. It appears that the electron-withdrawing 4′-Cl group enhances the acidity of the C_β–H bond to increase the extent of proton transfer, and stabilize the negative charge at the β-carbon, so that there is little change in the C_α–OAr bond cleavage.

Change of mechanism

The kinetic results described above clearly indicate that the reactant-like transition state for **1d** changes toward E2-central as a poorer leaving group is introduced (**1b**,**c**). When the leaving group ability is further decreased to X = H (**1a**), the E2 transition state is destabilized and the E1cb mechanism emerges simultaneously. The mechanism change also occurs by the β–aryl substituent, *i.e.*, from E2 for Ph_2CHCO_2Ar to concurrent E2 and E1cb mechanisms for **1a**. It is interesting to note that the mechanistic changes occur by the minor variations in the reactant structure.

We have previously reported that the mechanism of eliminations from aryl phenylacetates changes from E2 to E1cb *via* a competing E2 and E1cb mechanism.[17] The E2 transition state for this reaction was assumed to be E1cb-like and was located at E on the energy diagram, which is far from the position of the E1cb transition state (Fig. 2).[17] On the other hand, the E2 transition state for **1a** is similar to E2-central except that the extent of C_β–H bond cleavage is much larger. However, the position of the transition state (A) is significantly different from that of the E1cb transition state. To our knowledge, this is the first example that shows the change in the elimination mechanism from E2-central to a competing E2 and E1cb.

In conclusion, we have studied the ketene-forming eliminations from **1a**–**d** promoted by R_2NH–$R_2NH_2^+$ in 70 mol% MeCN (aq.). The reactions of **1b**–**d** proceed by a concerted E2 mechanism *via* an E2-central transition state. As the leaving group is made poorer, the E2 transition state becomes more skewed toward the proton transfer and the E1cb mechanism competes when X = H (**1a**). The mechanism of eliminations from Ph_2CHCO_2Ar is also changed from E2 to a competing E2 and E1cb by the electron-withdrawing β–aryl substituent. Noteworthy is the susceptibility of the ketene-forming transition state to the variation of the reactant structure.

Experimental

Materials

Aryl bis(4′-chlorophenyl)acetates (**1a**–**d**) were prepared from bis(4′-chlorophenyl)acetic acid and substituted phenols in the presence of Et_3N and 2-chloro-*N*-methylpyridinum iodide as previously reported.[15,19] The yield (%), melting points (°C), IR (KBr, C=O, cm^{-1}), NMR (300 MHz, $CDCl_3$), and combustion analysis data for the new compounds are as follows. Elemental analysis for **1d** could not be performed because it decomposed after several hours.

4-Nitrophenyl bis(4′-chlorophenyl)acetate (1a)

Yield 52%; mp 87–88 °C; IR 1757 (C=O); ^{1}H-NMR δ 5.21 (s, 1H), 7.25 (d, 2H, J = 9.2 Hz), 7.32 (d, 4H, J = 8.8 Hz), 7.38 (d, 4H, J = 8.8 Hz), 8.27 (d, 2H, J = 9.2 Hz). Anal. calcd for $C_{20}H_{13}Cl_2NO_4$: C, 59.72; H, 3.26; N, 3.48. Found: C, 59.68; H, 3.16; N, 3.42%.

2-Chloro-4-nitrophenyl bis(4′-chlorophenyl)acetate (1b)

Yield 42%; mp 85–87 °C; IR 1759 (C=O); ^{1}H-NMR δ 5.29 (s, 1H), 7.29 (d, 1H, J = 9.0 Hz), 7.35 (d, 4H, J = 8.8 Hz), 7.38 (d, 4H, J = 8.8 Hz), 8.17 (dd, 1H, J = 2.8 Hz and 9.0 Hz), 8.35 (d, 1H, J = 2.8 Hz). Anal. calcd for $C_{20}H_{12}Cl_3NO_4$: C, 55.01; H, 2.77; N, 3.21. Found: C, 55.08; H, 2.72; N, 3.12%.

2-Trifluoromethyl-4-nitrophenyl bis(4′-chlorophenyl)acetate (1c)

Yield 45%; mp 72–73 °C; IR 1765 (C=O); ^{1}H NMR δ 5.26 (s, 1H), 7.32 (d, 1H, J = 8.6 Hz), 7.38 (d, 4H, J = 8.6 Hz), 7.45 (d, 4H, J = 9.0 Hz), 8.46 (dd, 1H, J = 2.8 Hz and 9.0 Hz), 8.57 (d, 1H, J = 2.8 Hz). Anal. calcd for $C_{21}H_{12}Cl_2F_3NO_4$: C, 53.64; H, 2.57; N, 2.98. Found: C, 53.64; H, 2.53; N, 2.94%.

2-Nitro-4-nitrophenyl bis(4′-chlorophenyl)acetate (1d)

Yield 42%; mp 85–87 °C; IR 1759 (C=O); ^{1}H NMR δ 5.29 (s, 1H), 7.29 (d, 1H, J = 9.0 Hz), 7.35 (d, 4H, J = 8.8 Hz), 7.38 (d, 4H, J = 8.8 Hz), 8.17 (dd, 1H, J = 2.8 Hz and 9.0 Hz), 8.35 (d, 1H, J = 2.8 Hz).

Acetonitrile was purified as described previously.[15] The buffer solutions of R_2NH–$R_2NH_2^+$ in 70 mol% MeCN (aq.) were prepared by dissolving an equivalent amount of R_2NH and $R_2NH_2^+Cl^-$ in 70 mol% MeCN (aq.). In all cases, the ionic strength was maintained to 0.1 M with $Bu_4N^+Br^-$.

Kinetic studies

Reactions of **1a**–**d** with R_2NH–$R_2NH_2^+$ buffer in 70 mol% MeCN (aq.) were followed by monitoring the increase in the absorbance of the aryl oxides at 400–426 nm with a UV-vis spectrophotometer as described before.[26,27] Due to the instability of **1d** in MeCN, freshly prepared solution of **1d** was used in all kinetic runs.

Calculation of the k_2^E, k_1, and k_{-1}/k_2 values

Utilizing the k_{obs} values and the buffer concentration, the k_2^E, k_1, and k_{-1}/k_2 values that best fit with eqn. 2 have been calculated with the Origin program, which is a nonlinear square fitting routine based on the gradient search and function linearization method.[20]

Product studies

The products of eliminations from **1a**–**d** promoted by R_2NH–$R_2NH_2^+$ buffer in 70 mol% MeCN (aq.) were identified as reported.[15–17] The yields of the aryloxides determined by comparing the UV absorptions of the infinity samples with those for the authentic aryloxides were in the range of 90–98%.

H–D exchange experiment

To determine whether **1a** may undergo H–D exchange reaction, the substrates (0.19 mmol) were added to 3.4 mL of R_2NH–$R_2NH_2^+$ buffer (R_2NH = piperidine, 0.1 M) in 70 mol% MeCN–30% D_2O at −10 °C. The reaction was quenched and the reactant was isolated as described.[15–17] The proton NMR spectrum of the recovered reactant from **1a** was identical to that of the substrate except that the integration at δ 5.21 decreased by approximately 10%.

Control experiments

The stabilities of **1a**–**d** were determined as reported earlier.[15–17] Solutions of **1a**–**c** in MeCN were stable for at least 2 months in solution at room temperature. However, MeCN solution of **1d** was stable for only several hours.

Acknowledgements

This work was supported by Pukyong National University Research Foundation Grant in 2002.

References

1 B. Holmquist and T. C. Bruice, *J. Am. Chem. Soc.*, 1969, **91**, 2993–3002.
2 B. Holmquist and T. C. Bruice, *J. Am. Chem. Soc.*, 1969, **91**, 3003–3006.
3 R. F. Pratt and T. C. Bruice, *J. Am. Chem. Soc.*, 1970, **92**, 5956–5964.
4 M. Inoue and T. C. Bruice, *J. Am. Chem. Soc.*, 1982, **104**, 1644–1653.
5 M. Inoue and T. C. Bruice, *J. Org. Chem.*, 1982, **47**, 959–963.
6 A. William, *J. Chem. Soc., Perkin Trans. 2*, 1972, 808–812.
7 A. William and K. T. Douglas, *Chem. Rev.*, 1975, 627–649.
8 W. Tagaki, S. Kobayashi, K. Kurihara, K. Kurashima, Y. Yoshida and J. Yano, *J. Chem. Soc., Chem. Commun.*, 1976, 843–845.
9 T. J. Broxton and N. W. Duddy, *J. Org. Chem.*, 1981, **46**, 1186–1191.
10 R. Chandrasekar and N. Venkatasubramanian, *J. Chem. Soc., Perkin Trans. 2*, 1982, 1625–1631.
11 K. T. Douglas, M. Alborz, G. R. Rullo and N. F. Yaggi, *J. Chem. Soc., Chem. Commun.*, 1982, 242–246.
12 N. S. Isaac and T. S. Najem, *J. Chem. Soc., Perkin Trans. 2*, 1988, 557–562.
13 S. Y. Chung, S. D. Yoh, J. H. Choi and K. T. Shim, *J. Korean Chem. Soc.*, 1992, **36.**
14 K. Saigo, M. Usui, K. Kikuchi, E. Shimada and T. Mukaiyama, *Bull. Chem. Soc. Jpn.*, 1977, **50**, 1863–1866.
15 B. R. Cho, Y. K. Kim and C. O. Maing Yoon, *J. Am. Chem. Soc.*, 1997, **119**, 691–697.
16 B. R. Cho, N. S. Kim, Y. K. Kim and K. H. Son, *J. Chem. Soc., Perkin Trans. 2*, 2000, 1419–1422.
17 B. R. Cho, H. C. Jeong, Y. J. Seong and S. Y. Pyun, *J. Org. Chem.*, 2002, **67**, 5232–5238.
18 B. R. Cho, Y. K. Kim J. S. Yoon, J. C. Kim and S. Y. Pyun, *J. Org. Chem.*, 2000, **65**, 1239–1241.
19 K. Saigo, M. Usui, K. Kikuchi, E. Shimada and T. Mukaiyama, *Bull. Chem. Soc. Jpn.*, 1977, **50**, 1863–1866.
20 MacroCal Origin Version 3.5 MacroCal Software, Inc., Northamption, MA, 1991.
21 W. H. Saunders Jr and A. F. Cockerill, *Mechanism of Elimination Reactions*, Wiley, New York, 1973.
22 T. H. Lowry and K. S. Richardson, *Mechanism and Theory in Organic Chemistry*, Harper and Row, New York, 1987, pp. 591–616.
23 J. R. Gandler, *The Chemistry of Double bonded Functional Groups*, ed. S. Patai, John Wiley and Sons, Chichester, 1989, vol. 2, part 1, pp 734–797.
24 W. P. Jencks, *Chem. Rev.*, 1985, **85**, 511–527.
25 J. R. Gandler and W. P. Jencks, *J. Am. Chem. Soc.*, 1982, **104**, 1937–1951.
26 B. R. Cho, S. Y. Pyun and T. R. Kim, *J. Am. Chem. Soc.*, 1987, **109**, 8041–8044.
27 R. A. Bartsch and B. R. Cho, *J. Am. Chem. Soc.*, 1979, **101**, 3587–3591.